ELSEVIER

Surface Science 486 (2001) 82–94

SURFACE SCIENCE

www.elsevier.nl/locate/susc

Calculations of the energy accommodation coefficient using classical scattering theory

André Muis, J.R. Manson *

Department of Physics and Astronomy, Clemson University, Clemson, SC 29634, USA

Received 4 October 2000; accepted for publication 6 March 2001

Abstract

The theory of the energy accommodation coefficient for exchange of energy between a rarefied gas and a clean surface is developed in terms of the differential reflection coefficient for state-to-state scattering of an incoming atomic projectile and a surface. This theory is applied to classical models which have been shown to accurately predict the measured scattered distributions in numerous state-to-state experiments of monoenergetic beams of atoms scattering from clean single crystal surfaces and from clean liquid surfaces. Full three-dimensional calculations are carried out and compared with available experimental data for the accommodation of rare gases at a clean tungsten surface. Good agreement with the experimental measurements is obtained for the heavier mass rare gases where classical theory is expected to be most valid at all measured temperatures. © 2001 Elsevier Science B.V. All rights reserved.

Keywords: Noble gases; Atom–solid interactions, scattering, diffraction; Tungsten

1. Introduction

The modern theoretical basis of gas–surface studies began with the seminal work of Maxwell [1,2] and with Knudsen's 1910 analysis of the accommodation coefficient (AC) [3–6]. In the 1920s and 1930s there was considerable experimental activity led by the AC measurements of Roberts [7] and by the work of Stern and coworkers [8–13], who successfully demonstrated the quantum mechanical wave nature of atoms by diffraction from the highly corrugated surface of LiF. This experimental work prompted significant theoretical advances largely led by Lennard-Jones [14–17] and his coworkers such as Devonshire [18,19]. The next big advance in the field came in the late 1960s with the advent of modern high vacuum technology and the use of jet beams to produce well collimated and nearly monoenergetic atomic beams. This field of study has continued to advance to the point where atom–surface scattering, and in particular helium atom scattering, is a well developed technique of surface science [20]. Theoretical advances have kept pace with those in experiment and both the scattering theory and the theory of the interactions between atomic and molecular projectiles with crystalline and liquid surfaces are well developed [20–26].

During this same period, gas–surface scattering has developed considerably to the point where well-characterized and high-precision experiments can be carried out and compared with theory [27–34]. There is an area of common overlap between

* Corresponding author. Fax: +1-864-656-0805.

0039-6028/01/$ - see front matter © 2001 Elsevier Science B.V. All rights reserved.
PII: S0039-6028(01)01034-2

gas–surface interactions and atom–surface scattering and this is the domain of rarefied gas dynamics in which the gas pressure is sufficiently small that the molecular interactions with the surface occur as isolated events, which is the same condition under which typical atom–surface scattering experiments are carried out. Thus the state-to-state information obtained from an atom–surface scattering experiment can be used, after proper synthesis and averaging, to predict the characteristics of rarefied gas surface dynamics, e.g., energy transfer or drag and lift forces between a dilute gas and a surface. One of the most important and characteristic measures of gas–surface dynamics remains Knudsen's energy AC for which there is a large amount of high quality experimental data and numerous theoretical calculations [27].

The purpose of this paper is to re-examine the theory of the energy AC in the light of the many new advances in the classical and quantum theories of atom–surface scattering. In particular, we wish to incorporate recent theories of classical scattering [35–41] which have been shown to give excellent agreement with state-to-state measurements of atomic and molecular scattering off of crystalline and liquid surfaces.

The contents of this paper are as follows: in the next section (Section 2), the theory of the AC is developed in terms of a fully three dimensional reflection coefficient, the same reflection coefficient which is measured in an atom–surface experiment. In Section 3, several models for classical scattering from surfaces are discussed. In Section 4, details of the calculations are discussed and useful limiting cases for the AC and other quantities are derived, and Section 5 is a discussion of the behavior of the AC on the gas atom to surface atom mass ratio. In Section 6, full calculations of the ACs are compared with high quality data for the heat transfer of low pressure rare gases with a clean tungsten surface. Some conclusions from this work are considered in Section 7.

2. Theory

The energy AC is a measure of the actual energy exchanged between a gas initially placed in contact with a surface, and the maximum thermodynamically allowed energy which could be exchanged. Although the classic model for introducing the concept of energy accommodation is to have a gas initially in equilibrium with temperature T_G placed in contact with a surface which is initially in equilibrium at temperature T_S, many experiments are carried out for conditions in which the gas is in a highly non-equilibrium configuration, such as an incident molecular jet beam [42–48]. A convenient starting point is to consider the energy AC for a monoenergetic incident beam of atomic projectiles with energy E_i which may be defined according to

$$\alpha_E = \frac{\overline{E_f} - E_i}{\langle E_f \rangle - E_i} = \frac{\overline{E_f} - E_i}{2k_B T_S - E_i}, \tag{1}$$

where $\overline{E_f}$ is the average energy of an atomic particle after scattering from the surface. The notation $\langle E_f \rangle$ implies the average energy that an atom would have if it had scattered away in equilibrium with the surface at temperatures T_S, which for the Maxwell–Boltzmann distribution with the Knudsen flux correction is given by $\langle E_f \rangle = 2k_B T_S$ with k_B Boltzmann's constant. In more general experimental situations, the gas will be in an initial distribution of states and E_i must be replaced by the average over that distribution. In the case in which the gas is initially in a Maxwell–Boltzmann distribution then the AC becomes a function of two temperatures, that of both surface and initial gas given by

$$\alpha_E(T_S, T_G) = \frac{\overline{E_f} - \langle E_i \rangle}{\langle E_f \rangle - \langle E_i \rangle} = \frac{\overline{E_f} - 2k_B T_G}{2k_B T_S - 2k_B T_G}. \tag{2}$$

For theoretical simplicity it is convenient to define the equilibrium accommodation coefficient (EAC) $\alpha_E(T)$ as a function of a single temperature which is obtained as the limit in which surface and gas temperatures are the same, $T_G \to T_S \to T$.

$$\alpha_E(T) = \lim_{T_G \to T_S \to T} \alpha_E(T_S, T_G) = \lim_{T_G \to T_S \to T} \frac{\overline{E_f} - 2k_B T_G}{2k_B T_S - 2k_B T_G}. \tag{3}$$

The monoenergetic incident beam coefficient α_E of Eq. (1) has a distinct disadvantage in that it will

normally become undefined for the surface temperature at which its denominator vanishes. Despite this inconvenience, it is often useful as a measure of energy transfer between a beam and a surface [42,43]. On the other hand, the EAC $\alpha_E(T)$ remains well defined at all temperatures because the numerator and denominator both vanish linearly when $T_S \to T_G$, i.e., in this limit the average final energy $\overline{E_f}$ differs from $\langle E_i \rangle = 2k_B T_G$ only by a term which is linear in $T_S - T_G$.

For all of the above expressions (1)–(3) for the AC, the problem is reduced to one of determining the average energy of a gas projectile which has been scattered from the surface $\overline{E_f}$. In order to obtain this average energy it is convenient to introduce the concept of the differential reflection coefficient, which is the quantity usually measured in atom–surface scattering experiments. This is denoted by $dR(\mathbf{p}_f, \mathbf{p}_i, T_S)/dE_f d\Omega_f$ and is the probability per unit final energy and per unit solid angle that a particle of well-defined incident momentum $\mathbf{p}_i$ will be scattered into the small energy range dE_f and small solid angle $d\Omega_f$ centered about the final momentum $\mathbf{p}_f$. The condition of unitarity, or equality of total incident particle flux to total scattered flux, requires normalization of the differential reflection coefficient, i.e., the integral of $dR(\mathbf{p}_f, \mathbf{p}_i, T_S)/dE_f d\Omega_f$ over the energy and angles of all particles scattered from an incident beam of momentum $\mathbf{p}_i$ into the continuum plus the sum of all particles scattered from an incident beam of momentum $\mathbf{p}_i$ into the continuum plus the sum of all particles scattered into negative energy bound states is unity. The differential reflection coefficient specifies the angular and energy distributions of the scattered intensity, and it can be used to determine the average properties of the scattered flux.

The incident gas can be described by a distribution function $dP(\mathbf{p}_i, T_G)/dE_i d\Omega_i$ which, similar to the differential reflection coefficient, is also normalized to unity when integrated over all initial energies and over the 2π steradians of solid angle above the surface. For a well defined incident beam of momentum $\mathbf{p}_i$ this would be written as a product of Dirac δ functions in energy and solid angle, while for a flux-corrected Maxwell–Boltzmann distribution

$$\frac{dP^{MB}(\mathbf{p}_i, T_G)}{dE_i\, d\Omega_i} = \frac{E_i \cos\theta_i}{\pi (k_B T_G)^2} e^{-E_i/k_B T_G}, \tag{4}$$

where θ_i is the incident polar angle measured with respect to the normal to the surface.

The average final energy needed for calculating the double-temperature AC of Eq. (2) is consequently given by

$$\overline{E_f} = \int_0^\infty dE_i \int_{2\pi} d\Omega_i \int_0^\infty dE_f \int_{2\pi} d\Omega_f E_f \times \frac{dP^{MB}(\mathbf{p}_i, T_G)}{dE_i\, d\Omega_i} \frac{dR(\mathbf{p}_f, \mathbf{p}_i, T_S)}{dE_f\, d\Omega_f}. \tag{5}$$

A closed form expression can also be obtained for the EAC of Eq. (3) by exploiting the detailed balancing condition relating energy losses to energy gains that must be obeyed by the differential reflection coefficient. Detailed balancing between a direct scattering event in which a projectile strikes a surface initially at equilibrium and undergoes the state-to-state process $\mathbf{p}_i \to \mathbf{p}_f$ and the process $\mathbf{p}_f \to \mathbf{p}_i$ is expressed as

$$\frac{dR(\mathbf{p}_i, \mathbf{p}_f, T_S)}{dE_i\, d\Omega_i} = \frac{p_i \cos\theta_i}{p_f} \times \exp\left(\frac{E_f - E_i}{k_B T_S}\right) \frac{dR(\mathbf{p}_f, \mathbf{p}_i, T_S)}{dE_f\, d\Omega_f}. \tag{6}$$

This is a general result, equally applicable to both quantum and classical cases because the vibrational statistics of each phonon exchange at the surface are governed by the Bose–Einstein probability function which obeys this same detailed balancing relation. When the detailed balancing relation of Eq. (6) is used in conjunction with the average scattered energy of Eq. (5) the limit $T_G \to T_S$ of Eq. (3) can be carried out and the final result is

$$\alpha_E(T) = \frac{1}{4(k_B T)^2} \int_0^\infty dE_i \int_{2\pi} d\Omega_i \int_0^\infty dE_f \times \int_{2\pi} d\Omega_f (E_f - E_i)^2 \frac{dP^{MB}(\mathbf{p}_i, T)}{dE_i\, d\Omega_i} \times \frac{dR(\mathbf{p}_f, \mathbf{p}_i, T)}{dE_f\, d\Omega_f}. \tag{7}$$

Eq. (7), for a crystalline surface, involves a sixth order integral. If the surface can be considered azimuthally symmetric, such as the case for liquids or amorphous solids, then one of the azimuthal integrals becomes trivial and the problem reduces to a fifth order integral.

3. Scattering models

In the above section mathematical expressions for the energy ACs are presented in forms which are developed assuming that the differential reflection coefficient for state-to-state scattering of a single gas projectile is known. Numerous theoretical prescriptions have been presented for obtaining the differential reflection coefficient, both for the case of quantum mechanical scattering and classical scattering. In the case of classical atom–surface scattering, models have been developed for several different representations of surfaces which can be expressed as closed form mathematical equations. For the discussion of the AC in this paper, two of these classical models will be considered in detail.

The first of these models is the discrete model, in which the surface is regarded as a collection of discrete scattering centers at temperature T_S. For collision times short compared to typical vibration periods the single collision scattering of an atomic projectile is given by the following differential reflection coefficient [38,49,50]:

$$\frac{\mathrm{d}R^{(1)}}{\mathrm{d}\Omega_f\,\mathrm{d}E_f} = \frac{m^2|\mathbf{p}_f|}{8\pi^3\hbar^4 p_{iz} N_D}|\tau_{fi}|^2\left(\frac{\pi}{k_B T_S \Delta E_0}\right)^{1/2} \times \exp\left\{-\frac{(E_f - E_i + \Delta E_0)^2}{4k_B T_S \Delta E_0}\right\}, \tag{8}$$

where $\mathbf{p}_q$ is the momentum of a particle in state q, $\Delta E_0 = (\mathbf{p}_f - \mathbf{p}_i)^2/2M_c$ is the binary collision recoil energy, M_c is the surface atom mass, m is the projectile mass, N_D is the normalization factor, and $|\tau_{fi}|^2$ is the form factor of the scattering center. Eq. (8) has been applied to high energy inelastic neutron scattering [49], to low energy ion scattering [51,52], and to rare gas scattering from liquid metals [40].

If the surface is regarded as a flat continuous barrier, a somewhat different classical expression for single collision scattering is obtained [35–39]:

$$\frac{\mathrm{d}R^{(1)}}{\mathrm{d}\Omega_f\,\mathrm{d}E_f} = \frac{m^2 v_R^2|\mathbf{p}_f|}{4\pi^3\hbar^2 p_{iz} S_{u.c.} N_C}|\tau_{fi}|^2\left(\frac{\pi}{k_B T_S \Delta E_0}\right)^{3/2} \times \exp\left\{-\frac{(E_f - E_i + \Delta E_0)^2 + 2v_R^2 P^2}{4k_B T_S \Delta E_0}\right\}, \tag{9}$$

where $\mathbf{P}$ is the component of momentum exchange parallel to the surface $\mathbf{P} = \mathbf{P}_f - \mathbf{P}_i$, $S_{u.c.}$ is the area of a surface unit cell, N_C is the normalization factor. v_R, as specified by Brako and Newns [35], is the weighted average of sound velocities parallel to the surface and is expected to be of the order or less than the Rayleigh velocity of the solid. The Gaussian-like term involving v_R and $\mathbf{P}$ arises from scattering from vibrational correlations at the smooth surface. Eq. (9) has been used to describe the inelastic scattering of hyperthermal energy He atoms at energies above 0.1 eV from metal surfaces at temperatures above room temperature [53]. In this case the smooth continuous surface is due to the locus of classical turning points caused by the Pauli exchange repulsion with the low density of surface electrons extending outward from the bulk.

Up to this point the scattering data have been treated with a theory based on a purely repulsive interaction potential. However, the Van der Waals forces between the surface and the incident atomic projectile create an attractive well in front of the surface. In classical scattering, the primary effects of this adsorption well are to accelerate the incoming projectile and to refract the projectile into a trajectory that is directed more normal to the surface, and it provides channels for inelastic sticking. Since sticking is not considered in this work, the main effects of acceleration and refraction are correctly modeled by a simple attractive square well potential placed in front of the repulsive barrier. If the well is made wider than the selvage region of the surface then its width is unimportant, and the effect on the collision process is to replace the perpendicular components of the

momentum p_{qz} near the surface by an enhanced value $\tilde{p}_{qz}$ which includes the well depth D:

$$\tilde{p}_{qz}^2 = p_{qz}^2 + 2mD. \tag{10}$$

This model of the attractive potential refracts all projectiles at the leading edge of the well and causes them to collide with the barrier with a higher normal energy. Although the simple square-well model adopted here does not have the correct $1/z^3$ behavior of the leading term of the attractive Van der Waals potential, it does correctly produce the refraction effects and the higher energy of collision into the barrier caused by the well.

Not surprisingly, it is found that the adsorption potential well in front of the surface barrier plays a large role in shaping the scattered angular distribution when the incident energy is small [41]. The main effect of the inclusion of an attractive well, as compared to a potential with no well, is to broaden the scattered angular distribution lobes produced by a well defined incident beam when the incident energy is comparable to or not too much larger than the well depth.

The final quantity needed in order to specify the differential reflection coefficient is the form factor $|\tau_{fi}|^2$. A constant form factor is correct for classical hard-sphere scattering, and this is what we use for several of the calculations carried out below. The actual value of the constant is unimportant because that is fixed by the unitarity normalization of the differential reflection coefficient. Also, other choices of the form factor have been used. For example, a widely utilized form factor for elastic and inelastic He atom scattering is the Jackson–Mott form which is the quantum mechanical matrix element of an exponentially replusive potential, e.g., $V(z) = V_0 \exp(-\beta z)$, taken with respect to its own eigenfunctions [54]. In the semi-classical limit of a hard, repulsive barrier $\beta \to \infty$ this (and all other similar matrix elements) go to the limit [55]

$$\tau_{fi} = 4p_{fz}p_{iz}/m. \tag{11}$$

Eq. (11) will be referred to as the hard wall matrix element, and it is utilized in some of the calculations below.

4. Calculations and limiting cases

4.1. Discussion of numerical calculations

The numerical calculations which we report below in Section 6 use primarily the smooth-surface differential reflection coefficient of Eq. (9) and to some extent the discrete model of Eq. (8). The data which is used for comparison with the theoretical predictions comes from the high precision experiments of Thomas [56,57] and of Kouptsidis and Menzel [58,59] for rare gases in contact with a clean multicrystalline tungsten surface. Because the surface is multicrystalline it can be considered azimuthally symmetric with respect to the directions of the incident gas particles and this reduces the apparent sixth-order integral of the AC of Eq. (7) to a fifth-order integral. Since the classical differential reflection coefficients of Eqs. (8) and (9) are positive definite functions and, regarded as a function of final energy E_f for fixed incident momentum $\mathbf{p}_i$, consist of a peak with a single maximum, the integrals are ideally suited to integration algorithms using Gaussian quadratures. For all the five multiple integrals, a Guass–Laguerre quadrature was utilized together with an automatic check which increases the number of integration points until the desired precision was achieved. For small temperature differences $|T_S - T_G|$ the double temperature AC of Eq. (2) gave essentially identical results as the EAC of Eq. (7).

4.2. Limiting case

Evaluating analytically the theoretical expression for the EAC is a clearly non-trivial task except for the simplest models for the differential reflection coefficient, due to the large number of integrals. However, there is one case in which some interesting progress can be made, and this is the case of the discrete model of Eq. (8) at low temperatures and small mass ratio μ. In this limit the discrete model differential reflection coefficient, when regarded as a function of E_f for fixed E_i appears very similar to a Gaussian function, and in the limit the Gaussian function becomes very narrow and can approximate a Dirac δ function. This can be seen by regarding the Gaussian-like

exponential appearing in the discrete differential reflection coefficient of Eq. (8) as follows:

$$\exp\left(-\frac{(E_f - E_i + \Delta E_0)^2}{4k_B T_S \Delta E_0}\right) \approx \exp\left(-\frac{(E_f - f(\theta)E_i)^2}{4k_B T_S g(\theta) E_i}\right) \approx \sqrt{4\pi k_B T_S g(\theta) E_i}\,\delta(E_f - f(\theta)E_i), \quad (12)$$

where θ is the total scattering angle between final and initial momenta and $f(\theta)$ and $g(\theta)$s are given by [60]

$$f(\theta) = \left(\frac{\sqrt{1-\mu^2\sin^2\theta} + \mu\cos\theta}{1+\mu}\right)^2, \quad (13)$$

and

$$g(\theta) = \frac{\mu\left(1 + f(\theta) - 2\sqrt{f(\theta)}\cos\theta\right)}{\left(1 + \mu - \mu\cos\theta/\sqrt{f(\theta)}\right)^2}. \quad (14)$$

When the limiting expression of Eq. (12) is used in the discrete model differential reflection coefficient of Eq. (8) and inserted into the EAC of Eq. (7), the integral over E_f is trivially carried out using the δ function. Then the integral over E_i also becomes straightforward, and leads to

$$\alpha_E(T) \to \frac{3}{(1+\mu)^2}\int_{2\pi} d\Omega_i \frac{1}{N_D} \times \int_{2\pi} d\Omega_f [1 - f(\theta)]^2 h(\theta), \quad (15)$$

where

$$h(\theta) = \frac{\left[\sqrt{1-\mu^2\sin^2\theta} + \mu\cos\theta\right]^2}{\sqrt{1-\mu^2\sin^2\theta}}. \quad (16)$$

In this same limit the normalization for the discrete model becomes

$$N_D \to \frac{2\pi}{\cos\theta_i}\frac{1}{(1+\mu)^2}\int_{2\pi} d\Omega_f h(\theta). \quad (17)$$

This then leads to the somewhat simplified form

$$\alpha_E(T) \to \frac{3}{2} - \frac{3}{(1+\mu)^2}\int_{2\pi} d\Omega_i \frac{1}{N_D} \times \int_{2\pi} d\Omega_f f(\theta)[2 - f(\theta)]h(\theta). \quad (18)$$

For the continuum model differential reflection coefficient of Eq. (9) this limiting case cannot be so readily carried out, however, for small values of the parameter v_R such a limiting procedure can be effected.

5. Dependence of the equilibrium accommodation coefficient on mass ratio

There is a considerable body of work on establishing simple expressions for predicting the dependence of the EAC on the mass ratio $\mu = m/M_c$ [61,62]. Many of these arrive at equations based on the Baule expression for the energy transfer in a head-on collision between two hard spheres

$$E_f = \frac{4E_i\mu}{(1+\mu)^2}. \quad (19)$$

A very interesting derivation by Goodman, based on averaging the Baule expression (19) over classical trajectories, arrives at the following dependence of $\alpha_E(T)$ on μ [62]:

$$\alpha_E(T) \to \frac{2.4\mu}{(1+\mu)^2}. \quad (20)$$

It is of interest to compare the μ-dependence of the present calculational models with the simple expression of Goodman (20) and this is shown in Fig. 1. The short-dashed curve is the EAC calculated with the smooth-surface differential reflection coefficient of Eq. (9) with a constant form factor. The value of the velocity parameter was taken to be $v_R = 100$ m/s for this calculation, but the result is actually nearly independent of the value of v_R for v_R less than several thousand m/s. The long-dashed curve and the dotted curve are for the smooth-surface model with the hard wall form factor of Eq. (11) with $v_R = 1$ and 500 m/s, respectively. In contrast to the case with a constant form factor, when the parameter $v_R > 300$ m/s the value of the EAC begins to become smaller, and

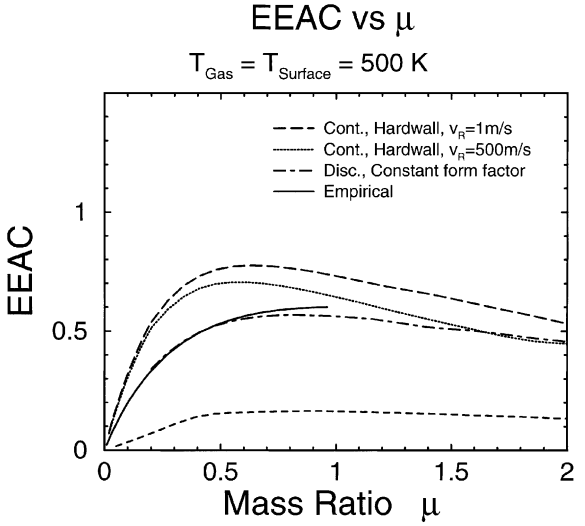

Fig. 1. The equilibrium energy accommodation coefficient $\alpha_E(T)$ as a function of mass ratio $\mu = m/M_c$ at a temperaure $T = 500$ K. The short-dashed curve is the calculation for the continuum model of Eq. (9) with a constant form factor, the long-dashed curve is for the continuum model with a hard wall form factor and $v_R = 1$ m/s, the dotted curve is the same with $v_R = 500$ m/s, the dash–dotted curve is for the discrete model of Eq. (8) with a constant form factor, and the solid curve is the empirical formula (20) of Goodman [62].

for $v_R = 500$ m/s there is a significant reduction at all expect the smallest mass ratios. The dash–dotted curve is the EAC calculated with the discrete differential reflection coefficient of Eq. (8) with a constant form factor. This is the zero-parameter model. The solid curve is Goodman expression of Eq. (20).

The discrete model calculation agrees well with the Goodman equation (20) for $\mu < 0.6$, which is perhaps not surprising since both are based on hard core scattering. It is interesting to note, however, that the Baule-based theories are valid only up to $\mu = 1$ because for $\mu > 1$ there is no backscattering when an incident hard sphere collides with a hard sphere of smaller mass. However, the discrete and smooth-surface scattering models of Eqs. (8) and (9) are valid for a larger range of μ. This is because these models correctly include the thermal motion of the target atoms, and backscattering events can occur even for $\mu > 1$ if the target is moving. As an example in fact, these models have been demonstrated to apply to the case of scattering of Xe atoms from a surface of the less massive metals Ga and In [40].

6. Comparison of calculations with measurements

In choosing a set of experimental measurements for initial comparisons with the present theory, one is impressed by the immense amount of data amassed on this subject since the seminal experiments by Roberts [7] in the 1930s. The overwhelming majority of this work has been reviewed in the important work of Saxena and Joshi [27]. Although the number of systems measured is large, clearly the most appropriate gases from the point of view of theoretical simplicity are the rare gases, and the most amenable surface to the constraints of the experimental conditions is the refractory metal tungsten. Since the experiments of Roberts, these rare-gas/tungsten system have been measured at several intervening periods with increasingly good surface cleanliness, to the point where now the accommodation of all the rare gases, with the exception of radon, have been measured [56,57] and verified over extended temperature ranges [58,59]. Clearly the rare-gas/tungsten system is the data of choice for which this theoretical work should be compared [55,63].

Our first calculation carried out for the EAC as a function temperature T used the discrete model of Eq. (8) with a constant form factor. This calculation is quite interesting because the model has no free parameters, thus it contains only kinematical and thermodynamical information with the interaction potential represented as a hard core interaction. Interestingly, the calculated EAC is very nearly a constant, independent of temperature, for each of the rare gases. The values of the EAC are very close to those given by the semi-empirical relation of Goodman in Eq. (20), as is evident from the mass ratio dependence shown in Fig. 1. The exception is the EAC for Xe which is calculated to be $\alpha = 0.553$ and the semi-empirical value is 0.583.

Fig. 2 shows a calculation for the smooth-surface differential reflection coefficient of Eq. (9) with a constant form factor. The α-coefficients for He, Ne, Ar, Kr and Xe are compared with the experi-

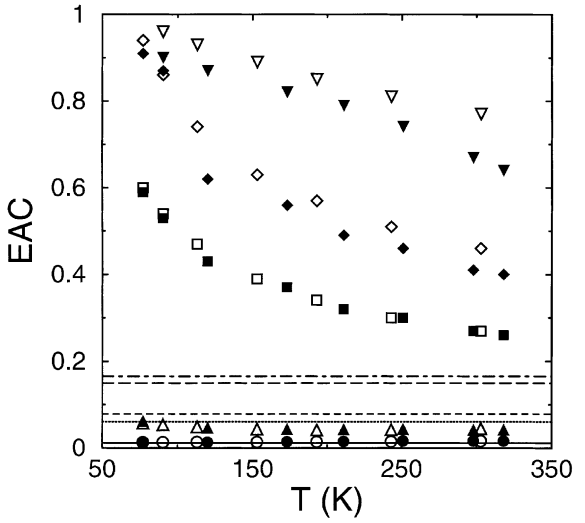

Fig. 2. The equilibrium energy accommodation coefficient $\alpha_E(T)$ as a function of surface temperature T for the five rare gases He, Ne, Ar, Kr and Xe on a W surface using the smooth-surface model of Eq. (9) with a constant form factor. The experimental data are those of Thomas [56,57] (open symbols) and of Kouptsidis and Menzel [58,59] (filled symbols). The data for He is shown as circles; Ne as triangles, Ar as squares, Kr as diamonds, and Xe as inverted triangles.

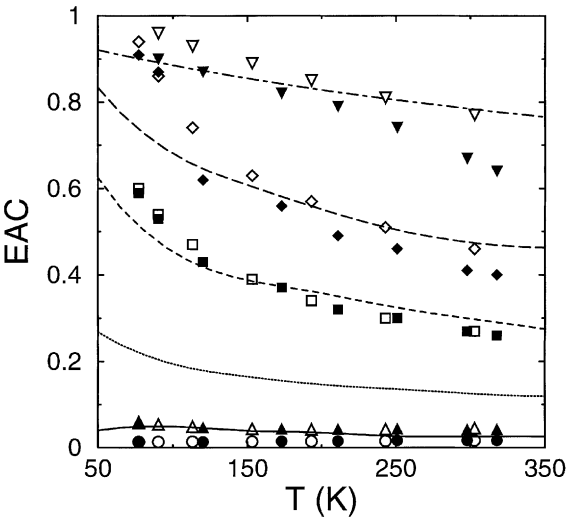

Fig. 3. The EAC for the rare gases in contact with a clean tungsten surface including the effects of the attractive adsorption potential well in front of the repulsive surface potential, plotted as a function of temperature for the smooth-surface model as in Fig. 2. The well depths are chosen as follows: He, 5 meV; Ne, 5 meV; Ar, 15 meV; Kr, 35 meV; and Xe, 300 meV and the average surface phonon velocity is taken as $v_R = 2500$ m/s.

mental data of Thomas [56,57] (open symbols) and of Kouptsidis and Menzel [58,59] (filled symbols). The data for He is shown as circles, Ne as triangles, Ar as squares, Kr as diamonds, and Xe as inverted triangles. The value chosen for $v_R = 100$ m/s, although as in Fig. 1 the results are independent of values of v_R in the range of up to several thousand m/s. Just as for the discrete model the calculated EACs are nearly independent of temperature. For both models this cannot be considered good agreement, although the AC values are correctly predicted to be increasing with the mass of the rare gas. However, these two calculations give a baseline for evaluating the EAC with relatively little, information on the potential. As we will show below in connection with Fig. 3, the discrepancy between the calculated values of the EAC and the experimental measurements appears to be mainly due to the absence of an attractive adsorption well in front of the repulsive part of the surface potential.

However, before examining the effects of the attractive well on the dynamics of the scattering process it is important to consider whether there could be measurable effects due to the absorption of the rare gas on the W surface at lower temperatures. The steady increase of the measured EAC values with decreasing temperature, especially for the heavier rare gases which have deep adsorption wells, might be attributed to an increasing residual adsorbed layer with decreasing temperature. Such a partial adsorbed layer would give rise to an increasing number of binary events with the incident gas particles scattering from other adsorbed rare gas atoms, events that have mass ratio $\mu = 1$ which maximizes the purely kinematical energy transfer at back scattering angles. The magnitude of such an effect can be estimated by calculating the rare gas adsorbate coverage Θ of the tungsten surface with the Langmuir isotherm [27]. Then the effects of adsorbates can be most readily estimated with the simple assumption that a fractional portion Θ of the surface is covered with rare gas adsorbates and the remaining fraction $1 - \Theta$ is clean W metal according to the following relation:

$$\alpha_E(T) = \Theta\alpha_E(T)_{\mu=1} + (1-\Theta)\alpha_E(T)_{\mu=m/M_C}, \qquad (21)$$

where $\alpha_E(T)_{\mu=1}$ is the AC for a surface of pure rare gas, and $\alpha_E(T)_{\mu=m/M_C}$ is the AC for scattering of a gas of mass m from the clean metal surface of mass M_C. The value of Θ calculated from the Langmuir isotherm depends on the adsorption energy (the depth of the adsorption well) and on the gas partial pressure. For reasonable values of these parameters corresponding to known experimental conditions, $\Theta(T)$ changes very rapidly from values near zero to values near unity over a range of temperature of just a few Kelvin. This sudden onset of adsorption, when used in Eq. (21), gives a nearly step-function increase in the value of $\alpha_E(T)$ at the adsorption transition temperature which is not at all similar to the gradual increase of the measured data at lower temperatures as seen in Fig. 2. This analysis indicates that adsorption of the gas is not the cause of the discrepancy between experiment and calculations in Fig. 2, and also indicates that it is not the cause of the gradual increase in $\alpha_E(T)$ at lower temperatures observed for the heavier rare gases.

Fig. 3 shows calculations of the EAC which take into account the attractive physical adsorption well of the surface potential. The theoretical curves are for the smooth-surface model of Eq. (9) with a parallel vibrational wave velocity $v_R = 2500$ m/s and a constant form factor. The well depths are chosen as He, 5 meV; Ne, 5 meV; Ar, 15 meV; Kr, 35 meV; and Xe, 300 meV. The reasonable agreement with experiment indicates that this is the effect that explains the gradual increase of the data with decreasing temperature for all except the lightest rare gases He and Ne. This behavior of the AC as a function of well depth has been discussed in detail previously by Goodman in the context of the theoretical models limiting the gas motion to one dimension [64–67]. There, it was shown that increasing the well depth both increases the AC values overall at all temperatures, and this increase becomes larger as the temperature decreases. The present fully three-dimensional model exhibits this same behavior as a function of well depth.

For comparison a list of calculated and measured values of the depths for the five rare gases on various amorphous or single crystal tungsten surfaces is given in Table 1 [68]. An examination of this table shows that there is little agreement on the values of these well depths, and for some gases the discrepancy is significantly greater than a factor of 2 between largest and smallest measured values. However, the values that we have used to fit calculations to the data in Fig. 3 tend to be smaller than the range of measured values.

Clearly, by using the well depth as a fitting parameter, the resulting calculations agree well with the experimental measurements for the heavier rare gases Xe, Kr and Ar for which the present classical model is expected to be valid. For the smaller mass elements Ne and He, the calculations with a non-zero well depth predict a value for $\alpha_E(T)$ which is significantly larger than the measured values. For a potential without a well, the AC values for He and Ne are in relatively good agreement with the data, as seen in Fig. 2, but as soon as even a small well depth is included the AC becomes too large.

These results for He and Ne stand in contrast to earlier calculations of Goodman using classical models limiting the gas motion to one dimension and taking the surface temperature to be always at absolute zero [66,67]. Goodman's results were in agreement with the data for reasonable values of the depths ($D = 6.0$ meV for He and $D = 27.3$ meV for Ne).

However, the large AC values found here for He and Ne with a non-zero well depth are expected, because the theoretical models are completely classical which means that they should apply only to heavier atomic gases. Helium at room temperature and below, interacting with metal surfaces, has been demonstrated to be a quantum mechanical system in which the energy exchange is dominated by single phonon transfers [20]. This quantum nature is even more pronounced with heavy metals such as platinum [69,70] and tungsten. For example, detailed He atom measurements of the dispersion relations for single crystal tungsten clearly show that the dominant inelastic processes for the scattering of thermal energy beams are single phonon transfers [84–86]. In fact, several single quantum theories of the EAC appear to explain the small values of $\alpha_E(T)$ measured for

Table 1
List of measured and calculated values for the well depths of the rare gases on multicrystalline tungsten and single crystal tungsten surfaces [68]

Gas–surface	D (meV)	Reference	Theoretical/ experimental
He–W	3.5	[71]	T
	4.3	[72]	E
	5	[P]	T
He–W(1 1 0)	3.5	[73]	E
	5.6[a]	[74]	E
He–W(1 1 2)	6.07	[75]	E
Ne–W(1 1 0)	17.4	[76]	E
	104	[77]	E
	5	[P]	T
Ar–W(1 1 1)	78.0	[78,79]	E
	82.5	[76]	E
	119	[80]	E
	46.6	[71]	T
	32.6	[81]	T
	127	[77]	E
	15	[P]	T
Kr–W	195	[82]	E
	239	[80]	E
	247	[77]	E
	35	[P]	T
Xe–W	180 ± 6	[83]	E
	300	[P]	T

Experimentally measured values are marked (E) and theoretical calculations are marked (T). The case of He–W(1 1 0) marked with the superscript a is the deepest quantum bound state. The entries referenced as [P] are the values used in this paper.

the He/W system [87–91]. Thus the classical theory developed here is not expected to give good quantitative results in the case of He. Similarly, for Ne there are ample numbers of experiments which have demonstrated that for interactions with metal surfaces both quantum mechanical diffraction [92–96] and single phonon inelastic events [97] are important. A theoretical study of the thermal attenuation of diffraction beams in Ne scattering from closed-packed Cu surfaces has shown that inelastic scattering over the range of temperatures and incident energies considered here can be explained with a combination of single and double phonon processes [98]. Thus, since both He/W and Ne/W are expected to be systems for which quantum effects are important it is expected that the present purely classical calculations, valid only when large numbers of phonon are transferred, overestimate the energy transfer and produce AC values that are too large.

7. Conclusions

We have developed a full three-dimensional theory of the AC under rarefied gas dynamics conditions in terms of the differential reflection coefficient for state-to-state scattering of gas particles from a clean surface. This theory is applied to two models of classical scattering of atomic projectiles at surfaces in the single-collision limit, the discrete model and the smooth-surface model. These two models have been previously demonstrated to give good quantitative predictions for the measured state-to-state scattered intensities in atom–surface experiments involving scattering of rare gases from metal, insulator and liquid surfaces. Thus they should be good predictors of the behavior of the AC.

Full three-dimensional calculations were carried out for comparison with the high-quality experimental data for the EAC for five different rare gases in contact with a clean, multi-crystalline tungsten surface. The parameter-free discrete model gave results which, although in the correct order of magnitude, are not in good agreement with experimental measurements. In fact, the EAC for this model was found to be nearly independent of temperature. However, this model is quite useful because it is totally free of adjustable parameters, it gives a baseline value of the EAC which contains only kinematics, and no specifics on the nature of the interaction potential between the projectile and the surface beyond a hard core interaction. The three-dimensional calculations using the somewhat more realistic smooth-surface model were in little better agreement with the data, and were also nearly independent of temperature.

However, good agreement with the data for the EAC of the heavy rare gases is obtained with the smooth-surface scattering model which includes the attractive adsorption well in the scattering potential and using the well depth as a fitting parameter. The importance of the attractive well and its influence on the shape of the AC has been

discussed earlier by Goodman [64–67] and these results confirm that the presence of a well increases the AC especially at low temperatures. The need to include the potential well has also been demonstrated for explaining the data for beams of the heavy rare gas atoms scattering from molten metals at low incident energies [41], in the same range of thermal energies encountered in measurements of the EAC. Similarly, the potential well is known to have important contributions to atom–surface scattering under quantum conditions [20]. This indicates the importance that the potential well plays in the process of energy exchange at a gas–surface interface.

The good agreement applied only to the heavy rare gases Ar, Kr and Xe. The smaller mass rare gases He and Ne have been shown in many previous experiments to behave as quantum scatterers in which energy exchange occurs only in single quanta or in small numbers of quanta. Since the calculations carried out here are entirely classical it is not surprising that the EAC for these small mass projectiles is overestimated. On the other hand, the heavy mass projectiles are expected to behave as fully classical projectiles, and this is supported by the agreement obtained with the present classical theoretical predictions.

Future work will involve including more details of the interaction potential between the gas particle and the surface, as well as investigating the effects of multiple collisions of the projectile with the surface. Also, comparisons will be made between these fully three-dimensional calculations and earlier calculations utilizing more restricted one-dimensional and two-dimensional models of the interaction potential in order to estimate the validity of such simpler and calculationally quicker approaches. Additionally, the importance of the attractive well indicates that sticking and temporary trapping in the adsorption states of the potential may play a role in the accommodation and energy exchange. The effects of transitions into the negative-energy bound (or adsorption) states of the potential will be investigated, including resonant transitions into the bound states. The sticking coefficient, which is very closely related to the AC [99,100], will also be investigated. In conclusion, it has been established that fully three dimensional calculations of the energy AC with suitably chosen parameters can explain the measured data over a large range of temperatures for the heavy rare gases Ar, Kr and Xe colliding with a W surface.

Acknowledgements

The authors like to express their appreciation to the Max Planck Institut für Strömungsforschung in Göttingen, Germany for hospitality during a portion of this work. This work was supported by the US Department of Energy under grant number DE-FG02-98ER45704 and by the National Science Foundation under grant number DMR-0089503.

References

[1] J.C. Maxwell, Phil. Mag. 19 (1860) 20.
[2] J.C. Maxwell, in: W.D. Niven (Ed.), The Scientific Papers of James Clerk Maxwell, vol. 2, Dover, New York, 1952, p. 706.
[3] M. Knudsen, Ann. Phys. 32 (1910) 809.
[4] M. Knudsen, The Kinetic Theory of Gases, Methuen, London, 1934.
[5] M. Knudsen, Ann. Phys. 48 (1915) 1113.
[6] M. Knudsen, Ann. Phys. 28 (1909) 999.
[7] J.K. Roberts, Proc. Roy. Soc. (London) A 129 (1930) 146.
[8] O. Stern, Z. Phys. 2 (1920) 49.
[9] O. Stern, Z. Phys. 3 (1920) 27.
[10] O. Stern, Z. Phys. 39 (1926) 751.
[11] F. Knauer, O. Stern, Z. Phys. 53 (1929) 766.
[12] I. Estermann, O. Stern, Z. Phys. 61 (1930) 95.
[13] I. Estermann, R. Frisch, O. Stern, Z. Phys. 73 (1931) 348.
[14] J.E. Lennard-Jones, A.F. Devonshire, Nature 137 (1936) 1069.
[15] J.E. Lennard-Jones, A.F. Devonshire, Proc. Roy. Soc. (London) A 156 (1936) 6.
[16] J.E. Lennard-Jones, A.F. Devonshire, Proc. Roy. Soc. (London) A 156 (1936) 29.
[17] J.E. Lennard-Jones, A.F. Devonshire, Proc. Roy. Soc. (London) A 158 (1937) 253.
[18] A.F. Devonshire, Proc. Roy. Soc. (London) A 156 (1936) 37.
[19] A.F. Devonshire, Proc. Roy. Soc. (London) A 158 (1937) 269.
[20] E. Hulpke (Ed.), Helium Atom Scattering from Surfaces, Springer Series in Surface Sciences, vol. 27, Springer, Berlin, 1992.
[21] V. Bortolani, A.C. Levi, Rivista del Nuovo Cimento 9 (1986) 1.

[22] J.P. Toennies, in: W. Kress, F.W. de Wette (Eds.), Springer Series in Surface Sciences, vol. 21, Springer, Heidelberg, 1991, p. 111.
[23] C.T. Rettner, M.N.R. Ashfold (Eds.), Dynamics of Gas–Surface Interactions, The Royal Society of Chemistry, Cambridge, 1991.
[24] S.A. Schaaf, P.L. Chambré, in: H.W. Emmons (Ed.), Flow of Rarefied Gases, High Speed Aerodynamics and Jet Propulsion 3, Section H, Princeton University Press, Princeton, NJ, 1958, pp. 687–739.
[25] W.R. Ronk, D.V. Kowalski, M. Manning, G.M. Nathanson, J. Chem. Phys. 104 (1996) 4842.
[26] L. Tribe, M. Manning, J.A. Morgan, M.D. Stephens, W.R. Ronk, E. Treptow, G.M. Nathanson, J.L. Skinner, J. Phys. Chem. 102 (1998) 206.
[27] S.C. Saxena, R.K. Joshi, Thermal accommodation and adsorption coefficients of gasses, in: C.Y. Ho (Ed.), CINDAS Data Series on Material Properties, Hemisphere, New York, 1989.
[28] H. Legge, Heat Transfer and Forces on a LiF Single-Crystal Disc in Hypersonic Flow, DLR-IB 222-92 A, vol. 14, DLR Göttingen, 1992.
[29] H. Legge, J.P. Toennies, J. Lüdecke, Proceedings of the 19th Rarefied Gas Dynamics Symposium, Oxford University, Oxford, 1994.
[30] H. Legge, J.P. Toennies, J.R. Manson, J. Chem. Phys. 110 (1999) 8767.
[31] C. Cercignani, in: D. Dini, C. Cercignani, S. Nocilla (Eds.), Rarefied Gas Dynamics, vol. 1, Editrice Technico Scientifica, Pisa, 1971, p. 75.
[32] C. Cercignani, M. Lampis, J. Appl. Math. Phys. 23 (1972) 713.
[33] C. Cercignani, M. Lampis, J. Appl. Math. Phys. 27 (1976) 733.
[34] C. Cercignani, M. Lampis, A. Lentati, On the drag and heat transfer coefficients in free molecular flow, Rarefied Gas Dynamics, vol. 2, Oxford University Press, Oxford, 1995, pp. 1190–1196.
[35] R. Brako, D.M. Newns, Phys. Rev. Lett. 48 (1982) 1859.
[36] R. Brako, D.M. Newns, Surf. Sci. 123 (1982) 439.
[37] H.-D. Meyer, R.D. Levine, Chem. Phys. 85 (1984) 189.
[38] J.R. Manson, Phys. Rev. B 43 (1991) 6924.
[39] J.R. Manson, Comput. Phys. Commun. 80 (1994) 145.
[40] A. Muis, J.R. Manson, J. Chem. Phys. 107 (1997) 1655.
[41] A. Muis, J.R. Manson, J. Chem. Phys. 111 (1999) 730.
[42] S.R. Cook, J.B. Cross, M. Hoffbauer, AIAA-94-2637, Proceedings of the 18th AIAA Aerospace Ground Testing Conference, 1994.
[43] G.E. Caledonia, R.H. Kreech, B.L. Upschulte, K.W. Holtzclaw, D.B. Oakes, AIAA-94-2638, Proceedings of the 18th AIAA Aerospace Ground Testing Conference, 1994.
[44] G.E. Caledonia, in: E.P. Muntz, D.P. Weaver, D.H. Campbell (Eds.), Rarefied Gas Dynamics: Space Related Studies, Progress in Astronautics and Aeronautics, vol. 116, AIAA, Washington, DC, 1989, pp. 129–142.
[45] G.E. Caledonia, R.H. Kreech, B.D. Green, AIAA J. 25 (1) (1987) 59.
[46] G.E. Caledonia, R.H. Kreech, B.L. Upschulte, D.M. Sonnenfroh, D.B. Oakes, K.W. Holtzclaw, AIAA 92-3974, Proceedings of the 17th Aerospace Ground Testing Conference, Nashville, 1992.
[47] R.H. Kreech, M.J. Gauthier, G.E. Caledonia, J. Spacecraft Rockets 30 (1993) 509.
[48] J.C. Gregory, P.N. Peters, in: V. Boffi, C. Cercignani (Eds.), Proceedings of the 15th International Symposium on Rarefied Gas Dynamics, Grado, Italy, 1986, pp. 644–656.
[49] A. Sjölander, Ark. Fys. 14 (1959) 315.
[50] D.A. Micha, J. Chem. Phys. 74 (1981) 2054.
[51] J. Hampton, C. Sosolik, unpublished.
[52] A. Muis, J.R. Manson, Phys. Rev. B 53 (1996) 2205.
[53] F. Hofmann, J.R. Manson, J.P. Toennies, Surf. Sci. 349 (1996) L184.
[54] J.M. Jackson, N.F. Mott, Proc. Roy. Soc. A 137 (1932) 703.
[55] F.O. Goodman, H.Y. Wachman, Dynamics of Gas–Surface Scattering, Academic Press, New York, 1976.
[56] L.B. Thomas, in: C.L. Brundin (Ed.), Rarefied Gas Dynamics, Academic Press, New York, 1967, p. 155.
[57] L.B. Thomas, in: H. Saltzburg, J.N. Smith, Jr., M. Rogers (Eds.), Fundamentals of Gas–Surface Interaction, Academic Press, New York, 1967, p. 346.
[58] J. Kouptsidis, D. Menzel, Berichte der Bunsen-Gesell. f. Phys. Chemie 74 (1970) 512.
[59] J. Kouptsidis, D. Menzel, Zeits. f. Naturforsch. 24a (1969) 479.
[60] A. Muis, J.R. Manson, Nucl. Instr. Meth. Phys. Res. B 125 (1997) 332.
[61] B. Baule, Ann. Physik 44 (1914) 145.
[62] F.O. Goodman, Surf. Sci. 7 (1967) 391.
[63] F.O. Goodman, H.Y. Wachman, Proc. Int. Sch. Phys. Enrico Fermi, Course LVIII, 1974, p. 491.
[64] F.O. Goodman, Phys. Chem. Solids 23 (1962) 1269.
[65] F.O. Goodman, Phys. Chem. Solids 24 (1963) 1451.
[66] F.O. Goodman, in: J.H. de Leeuw (Ed.), Rarefied Gas Dynamics, Academic Press, London, 1966, p. 366.
[67] F.O. Goodman, Prog. Surf. Sci. 5 (3) (1974) 261.
[68] G. Vidali, G. Ihm, H.-Y. Kimand, M. Cole, Surf. Sci. Rep. 12 (1991) 135.
[69] J.R. Manson, Surf. Sci. 272 (1992) 130.
[70] V. Celli, D. Himes, P. Tran, J.P. Toennies, Ch. Wöll, G. Zhang, Phys. Rev. Lett. 66 (1991) 3160.
[71] G.G. Kleiman, U. Landman, Solid State Commun. 18 (1976) 819.
[72] W.H. Weinburg, Ph.D. Thesis, University of Berkeley, 1971.
[73] W.H. Weinburg, J. Chem. Phys. 57 (1972) 5463.
[74] J.P. Cowin, C.F. Yu, S.J. Sibener, J.E. Hurst, J. Chem. Phys. 75 (1981) 1033.
[75] B. Salanon, J. Lapujoulade, Phys. Rev. B 36 (1987) 4428.
[76] G. Erlich, Brit. J. Appl. Phys. 15 (1964) 349.
[77] G. Oxinos, A. Modinos, Surf. Sci. 89 (1979) 292.

[78] R. Gomer, Aust. J. Phys. 13 (1960) 391.
[79] R. Gomer, J. Phys. Chem. 63 (1959) 468.
[80] T. Engel, R. Gomer, J. Chem. Phys. 52 (1970) 5572.
[81] R. Sau, R.P. Merrill, Surf. Sci. 34 (1973) 268.
[82] R.F. Steiger, J.M. Morabito, G.A. Somorjai, R.H. Miller, Surf. Sci. 14 (1969) 279.
[83] R. Opila, R. Gomer, Surf. Sci. 112 (1981) 1.
[84] H.-J. Ernst, E. Hulpke, J.P. Toennies, Phys. Rev. Lett. 58 (1987) 1941.
[85] H.-J. Ernst, E. Hulpke, J.P. Toennies, Europhys. Lett. 10 (1989) 747.
[86] E. Hulpke, J. Lüdecke, Phys. Rev. Lett. 68 (1992) 2846.
[87] R.T. Allen, P. Feuer, J. Chem. Phys. 43 (1965) 4500.
[88] F.O. Goodman, J. Chem. Phys. 56 (1972) 6082.
[89] F.O. Goodman, J.D. Gillerlain, J. Chem. Phys. 57 (1942) 3645.
[90] J.R. Manson, J. Chem. Phys. 56 (1972) 3451.
[91] B. Gaffney, J.R. Manson, J. Chem. Phys. 62 (1975) 2508.
[92] E. Semerad, P. Sequard-Base, E.M. Hörl, Surf. Sci. 189/190 (1987) 975.
[93] J.-P. Berthier, A. Constans, G. Daury, P. Lostis, Comptes Rendues Acad. Sci. Paris 278 (Serie B) (1974) 1067.
[94] E.K. Schwitzer, C.T. Rettner, Surf. Sci. 249 (1991) 335.
[95] G. Boato, P. Cantini, L. Mattera, Surf. Sci. 55 (1976) 141.
[96] B. Salanon, J. Physique 45 (1984) 1373.
[97] G. Armand, J.R. Manson, J. Physique 44 (1983) 473.
[98] G. Armand, J.R. Manson, C.S. Jayanthi, J. Physique (France) 47 (1986) 1357.
[99] T. Brunner, W. Brenig, Surf. Sci. 261 (1992) 284.
[100] A. Gross, W. Brenig, Surf. Sci. 289 (1993) 335.